

Frozen Quasi-Long-Range Order in the Random Anisotropy Heisenberg Magnet

M. Itakura

Center for Promotion of Computational Science and Engineering,
Japan Atomic Energy Research Institute, Taito-ku,
Higashiueno 6-9-3, Tokyo 110-0015, Japan

(Dated: October 30, 2018)

Extensive Monte Carlo simulations are used to investigate the low-temperature properties of the random anisotropy Heisenberg model, which describes the magnetic behavior of amorphous rare-earth-transition metal alloy. We show that the low-temperature phase in weak-anisotropy region is characterized by a *frozen-in* power-law spin-spin correlation. Numerical observation of the power-law exponent η indicates non-universal behavior.

PACS numbers: PACS numbers: 02.70.Lq, 75.10.Hk, 75.10.Nr

Note:

Owing to the page limitation, some parts of this manuscript are omitted in the published version. To obtain the published version, see the comments at the beginning of the TeX file.

Power-law correlation, or quasi-long-range order (QLRO), usually emerges just at the critical temperature of phase transition. The notable exception is the Kosterlitz-Thouless phase of two-dimensional XY model, in which power-law correlation persists down to zero temperature.¹ Recently it has been found that the low-temperature QLRO phase is quite common in disordered three-dimensional systems,² such as the so-called “Bragg-glass phase” of impure superconductors,^{3,4} nematic phase of liquid crystal in a porous media,^{5,6} and amorphous rare-earth-transition metal alloy.⁷ These systems are described either by random-field or random-anisotropy spin models. Harris, Plischke and Zuckermann first used the following random anisotropy model to study amorphous metal magnet⁸:

$$H = -J \sum_{\langle ij \rangle} \vec{S}_i \cdot \vec{S}_j - D \sum_i (\vec{n}_i \cdot \vec{S}_i)^2 \quad (1)$$

where \vec{S}_i is a Heisenberg spin on the lattice site i of simple cubic lattice, $J > 0$ is a ferromagnetic coupling constant, $D > 0$ is the strength of uniaxial anisotropy, the former sum runs over all nearest-neighbor pairs, and \vec{n}_i is a random unit vector which describes the random anisotropy at the site i . Similar model, in which $\vec{S}_i \cdot \vec{S}_j$ is replaced by $(\vec{S}_i \cdot \vec{S}_j)^2$, is used to study disordered liquid crystals. While an Imry-Ma-type argument⁹ of model (1) leads to a conclusion that any nonzero anisotropy D destroys long-range magnetic order in three dimensions, it is predicted by field theoretical analysis^{2,10,11} that the model realizes QLRO at low-temperature and weak-anisotropy region. The phase transition between this QLRO phase and paramagnetic phase is studied by ϵ -expansion techniques,¹² and it has been found that there are no renormalization group fixed point in a replica-transformed model of (1); usually this is interpreted as a sign of discontinuous transition, but no experiments report it. Numerical studies of model (1) have been

restricted to approximate discretized models or small sizes,^{13,14,15} and the QLRO phase was numerically confirmed in Ref.¹⁵. Similar phase was also found in the simulation of disordered liquid crystal.⁵ The possibility of spin-glass transition in the strong-anisotropy region has been investigated by Monte Carlo simulations, but no conclusive result has been obtained.^{13,14} Experimental studies have shown that there is a “spin freezing transition” below which zero-field cooled and field cooled magnetization differ.^{16,17} This phase is referred to as “correlated spin glass” phase,¹⁸ owing to the developed spin correlation length as opposed to the usual spin glasses. Similar glasslike behavior was found in the recent experiment of disordered liquid crystal.¹⁹ However, the predicted QLRO has not yet been reported experimentally.²⁰

In the present work, we numerically investigate the low-temperature properties of model (1) on an $L \times L \times L$ lattice for several values of D/J (including infinity) using the exchange Monte Carlo method.²¹ Details of the simulation are summarized in Table I: We simultaneously simulate N_r identical systems, assigning different temperature to each one. At each Monte Carlo step, exchange of states between adjacent temperatures T_i and T_{i+1} is tried and accepted with a probability $\min[1, \exp((E_i - E_{i+1})(1/T_i - 1/T_{i+1}))]$, where E_i denotes the energy of the state at T_i . Thus each state random-walks the temperature space. To maximize the diffusion constant of this process, a set of temperature $\{T_i\}$ is adjusted so that $(\langle E_{i+1} \rangle - \langle E_i \rangle)(1/T_{i+1} - 1/T_i) \sim -1$. The average energy can be easily estimated beforehand from simulations of smaller systems. Equilibrium is checked by dividing the measured data into groups and calculating averages for each group, then discarding the data of initial groups which are not equilibrated. In the Metropolis update of large D/J cases, the new spin is chosen with a probability proportional to $\exp(D/T(\vec{n}_i \cdot \vec{S}_i)^2)$ and acceptance probability is calculated using only the first term in 1. For small D/J cases, over-relaxation type update is also employed.²² When measuring the spin-glass order parameter, three replicas are placed at each temperature and overlaps between them are observed.

Note:

In the previous versions of this manuscript, the following observation scheme was used in some of exchange MC simulation. This scheme is incorrect, since the marked replica had always been at higher temperature just before it is observed, and average over such samples is biased to high-temperature side.

A special observation scheme is used when we investigate a large system at temperature far below the critical point: a replica is “marked” when it visits the highest temperature, and if a marked replica reaches the lowest temperature, we store its configuration into memory and “unmark” the replica. After MC steps proportional to N_R^2 , a large number of independent, equilibrium configurations at low temperature are obtained.

Average over random anisotropy configurations is performed over $48 \leq N_s \leq 900$ configurations. Statistical errors are estimated from sample-to-sample fluctuations by the Jackknife procedure. All the simulations were performed on Fujitsu VPP5000 vector processors at JAERI.

Fig.	D/J	L	T_{\min}/J	T_{\max}/J	N_R	MCS_I	MCS_O	N_S	
1	4.0	6	0.5	2.5	17	12000	12000	200	
		12	0.5	2.5	65	22500	22500	142	
		24	1.390	1.601	22	6000	4000	48	
2	4.0	24	0.832	1.601	91	6000	4000	96	
		10.0	6	0.5	2.5	17	12000	12000	400
			12	0.5	2.5	65	22500	22500	100
		24	0.969	1.930	61	60000	30000	80	
3	∞	8	0.5	2.5	17	12000	12000	900	
		12	0.5	2.5	33	24000	24000	600	
		20	0.754	1.665	42	48000	48000	176	
5	*	8	0.5	1.53 to 1.61	26	5000	10000	320	
		12	0.5	1.53 to 1.61	51	5000	40000	200 - 300	
		16	0.5	1.53 to 1.61	76	10000	70000	140 - 200	

TABLE I: Details of the exchange Monte Carlo simulations. N_R , MCS_I , MCS_O , and N_S denote number of replicas placed between T_{\min} and T_{\max} , number of Monte Carlo steps used for thermalization and discarded, number of Monte Carlo steps used for observations, and number of samples used for averaging over randomness, respectively. The sign “*” refers to all the values of D/J used in Fig. 5.

We observe both magnetization $\vec{m} = L^{-3} \sum_i \vec{S}_i$ and overlap parameter $q = L^{-3} \sum_i q_i$, where $q_i = \vec{S}_i^\alpha \cdot \vec{S}_i^\beta$ is an overlap at site i between two independent replicas α and β which we run in parallel. Figure 1 shows plots of Binder’s cumulant of \vec{m} and q :

$$B_m = \frac{5}{2} - \frac{3[\langle |\vec{m}|^4 \rangle]}{2[\langle \vec{m}^2 \rangle]^2}, \quad B_q = \frac{3}{2} - \frac{[\langle q^4 \rangle]}{2[\langle q^2 \rangle]^2} \quad (2)$$

for the $D/J = 4.0$ case, where $\langle \dots \rangle$ and $[\dots]$ denote thermal and sample averages, respectively. A clear crossing at $T \approx 1.423$ can be observed for both B_m and B_q which

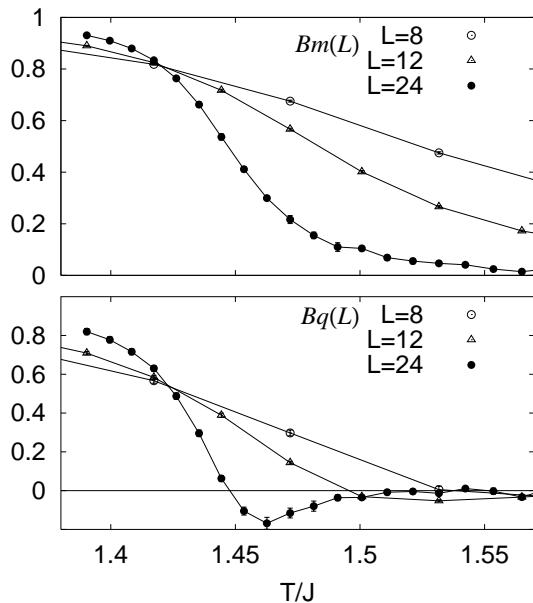


FIG. 1: Plots of B_m and B_q for the $D/J = 4.0$ case.

clearly indicates that there is some kind of order at low temperatures (Note that the transition temperature is only 2% smaller than that of $D = 0$ case, as was found in Ref. ¹⁵). To investigate the nature of the ordered phase, we observe the effective exponent of η defined between two different system sizes L_1 and L_2 :

$$2 - d - \eta_{\text{eff}} = \frac{\ln[\langle \vec{m}(L_2)^2 \rangle] - \ln[\langle \vec{m}(L_1)^2 \rangle]}{\ln(L_2) - \ln(L_1)}, \quad (3)$$

where d denotes spatial dimension (in the present case, $d = 3$). When spin-spin correlation at a distance r is proportional to $r^{2-d-\eta}$, then η_{eff} asymptotically approaches to η as the size is increased, while when the correlation is short ranged, $[\langle \vec{m}^2 \rangle]$ is proportional to L^{-d} , therefore $\eta_{\text{eff}} = 2$ is approached. Figure 2 shows plots of η_{eff} for the $D/J = 4.0$ case: The value of η_{eff} is almost independent of temperature below the critical point. This behavior is quite different from that of Kosterlitz-Thouless (KT) phase,¹ in which η_{eff} jumps from 2 to 1/4 at the critical point, then gradually decreases down to 0 as the temperature is lowered down to $T = 0$. The difference from the KT phase becomes remarkably clear when one sees a probability distribution of the overlap parameter $P(q') = [\langle \delta(q - q') \rangle]$. The inset of Fig. 2 shows $P(q)$ of two sizes $L = 8$ and 12, for the $D/J = 4.0$ case, at a very low temperature $T/J = 0.6815$ which is well below the critical point; the sharp peaks, which become sharper as the size is increased, indicate that only one kind of state is dominant in the ordered phase and there are no critical thermal fluctuations. From these results, one can depict the nature of the low-temperature phase as follows: the system is trapped around one of the two ground states $\pm \{\vec{S}_i^{(0)}\}$, in which spin-spin correlation decays as $\vec{S}_i^{(0)} \cdot \vec{S}_j^{(0)} \sim |i-j|^{-\eta-1}$. At the transition tempera-

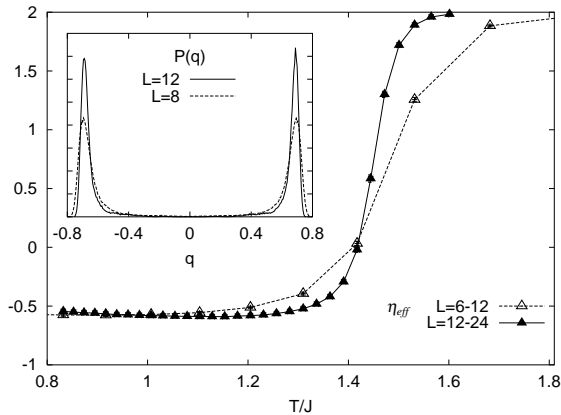


FIG. 2: Plots of the effective exponent η_{eff} against temperature for the $D/J = 4.0$ case. Statistical errors are smaller than the size of the symbols. The inset shows probability distribution of the overlap parameter q at $D/J = 4.0$, $T/J = 0.6815$.

ture, the system “freezes” into this QLRO state, then the magnetic QLRO and the spin-glass order simultaneously emerge. Baker and Kadanoff suggested similar QLRO phase for models with finite zero-point entropy, such as antiferromagnetic Potts models, in which thermal fluctuation is present even at $T = 0$. They speculated that in these models the point $T = 0$, along with the whole low-temperature phase, is renormalized to some nontrivial fixed point. But in the present case, the behavior of $P(q)$ suggests that there is only one kind of low-temperature state and thermal fluctuation is irrelevant in the low-temperature phase.

Next, we consider the low-temperature phase in the strong-anisotropy region, in which QLRO is expected to be destroyed.^{13,14} Figure 3 and 4 shows plots of B_m and B_q for $D/J = 10$ and $D/J = \infty$ cases, respectively. The case $D/J = \infty$ correspond to a kind of Ising spin-glass model $\sum_{\langle ij \rangle} J_{ij} \sigma_i \sigma_j$ with $J_{ij} = \vec{n}_i \cdot \vec{n}_j$. The plots of B_m shown in Fig. 3 and 4 do not show crossing behavior and are consistent with the past results, and indicate that the spin-spin correlation is already short ranged at $D/J = 10$. As for the spin-glass order, however, the crossing of the plots of B_q is rather ambiguous; they seem to collapse into a line in the low-temperature region. This result is suggestive of Kosterlitz-Thouless-like *quasi-long-ranged spin-glass order*, but it should be remembered that numerical simulations of the three-dimensional $\pm J$ spin glasses could not exclude a (false) possibility of KT-like transition, unless recently large-scale simulations have become possible.²³ So, in the present work we reserve conclusion on this issue. The phase diagram shown in Fig. 5 summarizes these results. In the weak-anisotropy limit, magnetic order is either slowly decaying QLRO or long ranged, which is difficult to distinguish numerically.

Now let us consider the following question: Is the exponent η universal all over the QLRO phase? The field

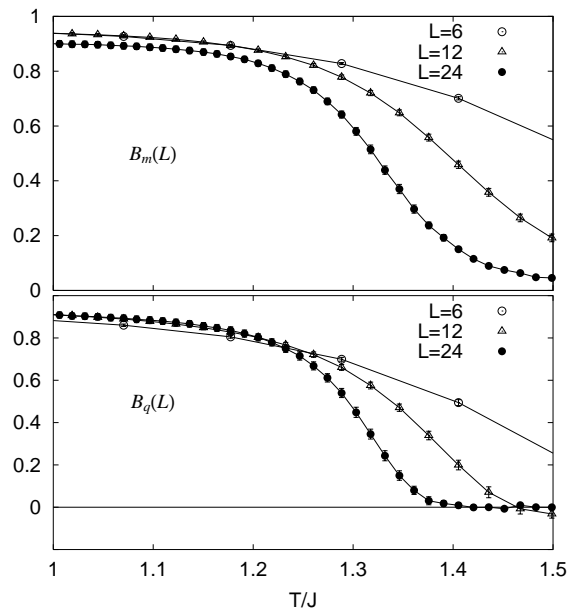


FIG. 3: Plots of B_m and B_q for the $D/J = 10.0$ case.

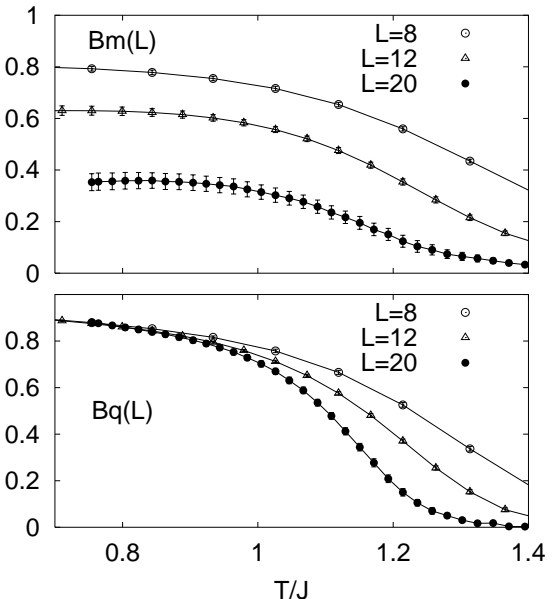


FIG. 4: Plots of B_m and B_q for the $D/J = \infty$ case.

theoretical $4 - \epsilon$ expansion analysis^{2,11} suggests that a stable fixed point at $D/J = O(\epsilon)$ governs the nature of the whole QLRO phase. Figure 6(a) schematically depicts the finite-size behavior of η_{eff} expected from this theoretical framework. Although the $4 - \epsilon$ expansion analysis only foretells the presence of a stable RG fixed point, there should be another, an unstable fixed point since the QLRO is destroyed in the strong-anisotropy limit. When the anisotropy ratio D/J is smaller than a threshold (unstable fixed point), it is attracted to a stable fixed point as it is renormalized, while it will diverge when larger

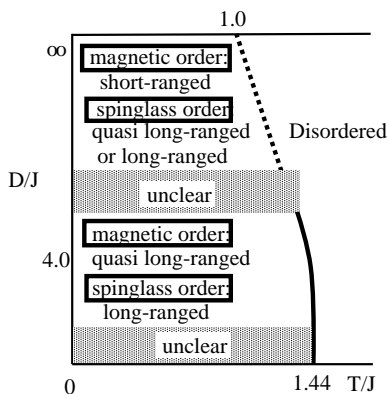


FIG. 5: Phase diagram of the random anisotropy magnet, suggested by the results of the present work. Dotted lines and shaded area are ambiguous phase boundaries which are hard to identify by numerical simulations.

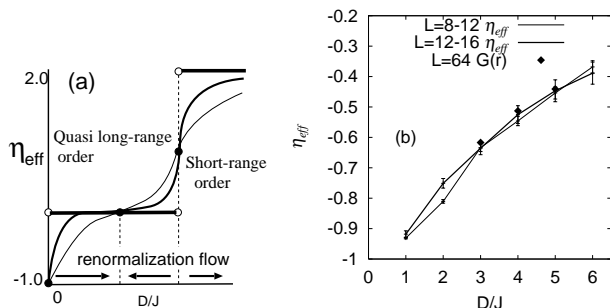


FIG. 6: (a) Schematic representation of finite-size behavior of the effective exponent η_{eff} expected from renormalization-group analysis. Thin and thick curves are finite-size values of smaller and larger systems, respectively. The bold straight lines show the infinite-volume limit. (b) Effective exponent η_{eff} of several values of D/J , measured at $T/J = 0.5$ for all cases. The data represented by a dotted line are calculated from correlation function of spin configurations obtained by simulated annealing of $L = 64$ system.

than the threshold. Thus plots of η_{eff} against D/J at a low temperature for different sizes will intersect at two fixed points. Figure 6(b) shows plots of η_{eff} measured at a very low temperature $T/J = 0.5$ (far below the transition line $T \sim 1.4$) for several values of D/J and for different sizes. In a region $3.0 \leq D/J \leq 6.0$, the two plots coincide within statistical errors, unlike Fig. 6(a). This suggests a nonuniversal QLRO phase in which the asymptotic value of η continuously changes with varying D/J , or at least that the renormalization-group flow is very slow.

To see if the observed nonuniversal QLRO is asymptotic or not, we investigate larger system $L = 64$ with simulated annealing (SA) method.²⁴ The apparent drawback of SA is that it does not guarantee equilibration, therefore obtained configuration may not be the true ground state. Energy of the obtained states is given in

Table II.

D/J	3.0	4.0	5.0	6.0	8.0	10.0
E_0	-4.7099	-5.5617	-6.4705	-7.4082	-9.3314	-11.2871
ΔE_0	± 0.0004	± 0.0004	± 0.0005	± 0.0005	± 0.0007	± 0.0005

TABLE II: Energy per spin of the annealed states, averaged over randomness. The third row shows standard deviation of sample-to-sample fluctuations.

Using the configurations obtained by SA, we calculate spin correlation function defined as $G(r) \equiv (3L^3)^{-1} \sum_{|i-j|=r} \vec{S}_i \cdot \vec{S}_j$, where the summation runs over all pairs whose relative position is either $(r, 0, 0)$, $(0, r, 0)$, or $(0, 0, r)$ lattice spacings. For each random anisotropy configuration, only one annealed configuration is generated and $G(r)$ is averaged over ten random anisotropy configurations. The summation over lattice sites significantly reduces statistical errors, and this small number of random anisotropy configurations is enough to obtain reasonable precision. Figure 7 shows plots of $G(r)$ for various values of D/J . For the cases of $D/J \leq 4.0$, $G(r)$ in a range $4 \leq r \leq 16$ is well fitted by a power-law form $G(r) = ar^{-\eta-1}$, while for $D/J \geq 5.0$ a form $G(r) = ar^{-\eta-1} \exp(-x/\xi)$ is well fitted. Owing to the periodic boundary condition, the data in a region $r > 16$ deviate from the fitting forms. The values of η for each D/J obtained by the fitting are shown in Fig. ??, and they coincide with the previous results within statistical errors. The inset of Fig. 7 shows plot of η and $1/\xi$ against D/J : $G(r)$ becomes short ranged at around $D/J = 5.0$, therefore the QLRO phase should persist at least up to this anisotropy strength.

Now that we have found a QLRO phase at around $D/J = 4.0$, which is much larger than that of experimentally realized materials $D/J \sim 1.0$, a question arises: Why has this QLRO phase never been observed in the past experiments, such as small angle neutron scattering²⁰? One possible reason may be the temperature dependence of the anisotropy D : Generally D increases as the temperature is lowered, while J remains almost constant.¹⁸ Since the ground state is completely modified when D/J changes, reaching the true ground state requires complete reorganization of spins, which is unlikely to happen no matter how slowly the system is cooled.

In summary, we have carried out extensive Monte Carlo simulations of the three-dimensional random anisotropy Heisenberg model and found a QLRO phase which is characterized by frozen power-law spin correlations in the low-temperature, weak-anisotropy region. This phase persists at least up to the anisotropy strength $D/J \approx 5.0$. Finite-size behavior of the effective power-law exponent in this phase indicates nonuniversal behavior, contrary to the field theoretical prediction of universal exponent.

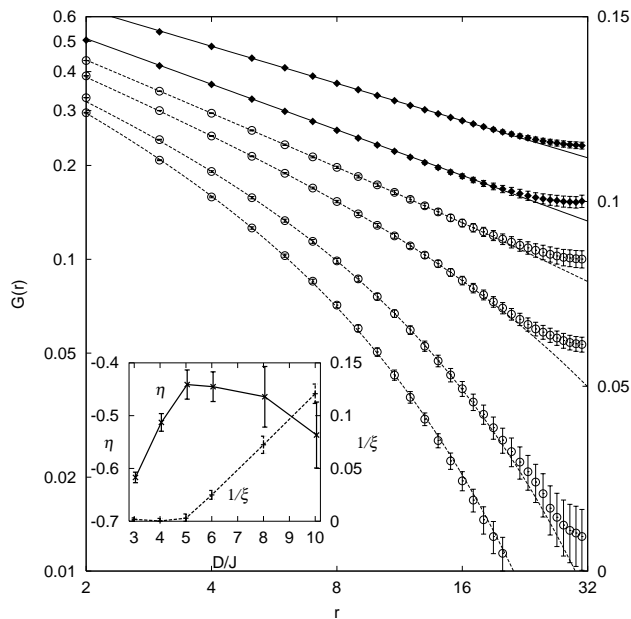


FIG. 7: Spin-spin correlation $G(r)$ in the annealed states for $D/J = 3.0, 4.0, 5.0, 6.0, 8.0,$ and 10.0 cases (from top to bottom), averaged over ten samples for each case. Lines are results of fittings, either $G(r) = ar^{-\eta-1}$ (solid lines) or $G(r) = ar^{-\eta-1} \exp(-r/\xi)$ (dotted lines). The inset shows plot of the fitting parameter η and $1/\xi$ against D/J .

-
- ¹ J.M. Kosterlitz and D.J. Thouless, *J. Phys. C* **6**, 1181 (1973); J.M. Kosterlitz, *ibid.* **7**, 1046 (1974).
² D.E. Feldman, *Int. J. Mod. Phys. B* **15**, 2945 (2001).
³ T. Klein, I. Joumard, S. Blanchard, J. Marcus, R. Cubitt, T. Giamarchi, and P. Le Doussal, *Nature (London)* **413**, 404 (2001).
⁴ T. Giamrachi and P. Le Doussal, in *Spin Glasses and Random Fields* (Ref.²³).
⁵ J. Chakrabarti, *Phys. Rev. Lett.* **81**, 385 (1998).
⁶ D.E. Feldman, *Phys. Rev. Lett.* **84**, 4886 (2000).
⁷ K. Moorjani and J.M.D. Coey, *Magnetic Glasses* (Elsevier, New York, 1984).
⁸ R. Harris, M. Plischke, and M.J. Zuckermann, *Phys. Rev. Lett.* **31**, 160 (1973).
⁹ R.A. Pelcovits, E. Pytte, and J. Rudnick, *Phys. Rev. Lett.* **40**, 476 (1978).
¹⁰ A. Aharony and E. Pytte, *Phys. Rev. Lett.* **45**, 1583 (1980).
¹¹ D.E. Feldman, *Phys. Rev. Lett.* **84**, 4886 (2000); *Phys. Rev. B* **61**, 382 (2000).
¹² M. Dudka, R. Folk, and Yu. Holovatch, *Fluctuating Paths and Fields*, edited by W. Janke, A. Pelster, H.-J. Schmidt, and M. Bachmann, (World Scientific, Singapore) p. 457-467, preprint cond-mat/0106334.
¹³ C. Jayaprakash and S. Kirkpatrick, *Phys. Rev. B* **21**, 4072 (1980).
¹⁴ R. Fisch, *Phys. Rev. B* **42**, 540 (1990).
¹⁵ R. Fisch, *Phys. Rev. B* **58**, 5684 (1998).
¹⁶ B. Dieny and B. Barbara, *Phys. Rev. Lett.* **57**, 1169 (1986).
¹⁷ D.J. Sellmyer and S. Nafis, *Phys. Rev. Lett.* **57**, 1173 (1986).
¹⁸ E.M. Chudnovsky, W.M. Saslow, and R.A. Serota, *Phys. Rev. B* **33**, 251 (1986).
¹⁹ T. Bellini, M. Buscaglia, C. Chiccoli, F. Mantegazza, P. Pasini, and C. Zannoni, *Phys. Rev. Lett.* **88**, 245506 (2002).
²⁰ A.C. Hannon, M. Hagen, R.A. Cowley, H.B. Stanley and N. Cowlam, *Physica B* **180-181**, 230 (1992).
²¹ K. Hukushima and K. Nemoto, *J. Phys. Soc. Jpn.* **65**, 1604 (1996).
²² M. Caselle and M. Hasenbusch, *J. Phys. A* **31**, 4603 (1998).
²³ *Spin Glasses and Random Fields*, edited by A. P. Young (World Scientific, Singapore, 1997).
²⁴ S. Kirkpatrick, C. D. Jr. Gelatt and M. P. Vecchi, *Science* **220**, 671 (1983).